GEOPHYSICAL RESEARCH LETTERS, VOL. 27, NO. 3, PAGES 401-404, FEBRUARY 1, 2000

Sensitivity of the Antarctic sea ice to the thermal conductivity of snow

Thierry Fichefet, Benoît Tartinville, and Hugues Goosse

Institut d'Astronomie et de Géophysique G. Lemaître, Université Catholique de Louvain, Louvain-la-Neuve, Belgium

Abstract. The sensitivity of a global, coarse-resolution ice-ocean model to a decrease in the thermal conductivity of the snow overlaying Antarctic sea ice (k_{sant}) is investigated. This study was motivated by recent observations made in the eastern sector of the Southern Ocean and in the Bellingshausen, Amundsen, and Ross Seas, which suggest that the value of k_{sant} usually used in large-scale sea ice models is about a factor two too high. When k_{sant} is reduced by half in our model, the average thickness of the Antarctic ice pack decreases by 10 cm (10%) and the geographical distributions of snow and ice thicknesses become more realistic. A strengthening of the Southern Ocean stratification and a concomitant weakening of the Antarctic Bottom Water meridional overturning are also noticed. This ultimately impacts on the sensible heat flux from the ocean to the ice and thus on the rate of thermodynamic ice growth.

1. Introduction

Snow that accumulates on top of sea ice can significantly affect the thermodynamic growth and decay of the ice cover. Because of its low thermal conductivity, the snow cap acts as an insulating blanket that curtails the conduction of heat from the ice bottom to the interface with the atmosphere, thus slowing down basal ice growth. Besides, owing to its high albedo, the snow cover acts as a protective screen against incoming shortwave radiation, retarding or even frustrating the onset of surface melting. The fact that snow has to melt away before surface ablation of the ice underneath occurs further delays the beginning of surface ice melting. In addition to these effects, snow can actively contribute to ice thickening through the process of snow ice formation.

Since the pioneering works of *Maykut and Untersteiner* [1971] and *Semtner* [1976], a value of 0.31 W m^{-1} K^{-1} has been used for the thermal conductivity of snow in the majority of large-scale sea ice models. Recent field measurements of snow characteristics have been carried out on East Antarctic sea ice [*Massom et al.*, 1998] and in the Bellingshausen, Amundsen, and Ross Seas [*Sturm et al.*, 1998]. Analysis of the collected data yields an average value for the thermal conductivity of the Antarctic snow pack (k_{sant}) which is about half the generally adopted value. Given the importance of the insulating effect of snow for Antarctic sea ice [see, e.g., *Owens and Lemke*, 1990; *Ledley*, 1991; *Eicken et al.*, 1995; *Fichefet and Morales Maqueda*, 1997, 1999; *Wu et al.*, 1999], it is urgent to investigate to what extent such a change in k_{sant} alters the Antarctic sea ice simulations.

Wu et al. [1999] have shown that diminishing k_{sant} by half in their atmosphere–sea ice general circulation model induces a thinning of the Antarctic ice cover of 20 cm (27%), on average, and a reduction in ice extent of 2.5×10^6 km^2 (42%) at the time of the seasonal minimum. However, in their study, the oceanic heat flux at the ice bottom was prescribed, which precluded any oceanic feedback. Actually, the decrease in the rate of thermodynamic ice growth resulting from the enhanced insulating effect of snow should induce a reduction in the rate of brine rejection into the ocean. This in turn could affect the ocean structure and dynamics, and therefore the heat exchange at the ice-ocean interface.

Here we repeat the sensitivity experiment conducted by *Wu et al.* [1990] with a global, coarse-resolution ice-ocean model. As our model is not coupled to an atmospheric model, this investigation must be viewed as complementing the one by *Wu et al.* [1999].

2. Model, Forcing, and Experimental Design

The model utilized in this work is identical to that of *Goosse and Fichefet* [1999] (hereafter referred to as GF). It is made up of a primitive-equation, free-surface ocean general circulation model coupled to a thermodynamic-dynamic sea ice model with viscous-plastic rheology. The oceanic component includes a parameterization of vertical mixing based on the *Mellor and Yamada* [1982] level-2.5 turbulence closure scheme. The sea ice component takes into account the presence of snow on top of sea ice, the storage of sensible and latent heat inside the snow-ice system, the influence of the subgrid-scale snow and ice thickness distributions on sea ice thermodynamics, and the transformation of snow into snow ice when the snow-ice interface sinks below the water line (see *Fichefet and Morales Maqueda* [1997] for details). The horizontal resolution is of 3° × 3°, and there are 20 vertical levels in the ocean, with 6 levels in the top 100 m.

The model is dynamically driven by the climatological monthly wind stresses of *Hellerman and Rosenstein* [1983] between 15° N and 15° S and of *Trenberth et al.* [1989] out of this region. The surface fluxes of heat are determined from atmospheric data by using classical bulk formulas. Input fields consist of climatological monthly surface air temperatures [*Taljaard et al.*, 1969; *Crutcher and Meserve*, 1970] and relative humidities [*Trenberth et al.*, 1989], cloud fractions [*Berliand and Strokina*, 1980], and surface winds (same sources as for wind stress). Evaporation/sublimation is derived from the turbulent flux of latent heat. Precipitation and freshwater inflow from the largest rivers are prescribed according to the monthly climatologies of *Xie and Arkin*

Paper number 1999GL002397.
0094-8276/00/1999GL002397$05.00

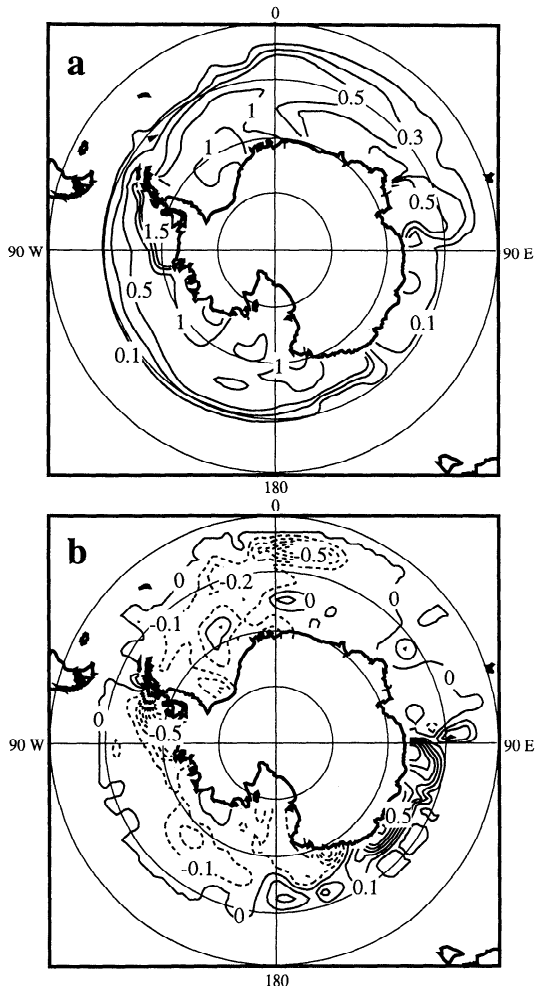

Figure 1. (a) Antarctic sea ice thicknesses from CTRL for September. Selected contours are 0.1, 0.3, 0.5, 1.0, 1.5, and 2.0 m. (b) Differences in Antarctic sea ice thickness between LC and CTRL for September. Contour interval is 0.1 m.

[1996] and *Grabs et al.* [1996], respectively. For the small rivers, the annual runoff values of *Baumgartner and Reichel* [1975] are utilized. In addition to this forcing, a relaxation toward observed annual mean salinities [*Levitus*, 1982] is applied in the 10-m-thick surface grid box outside polar regions with a time constant of 2 months. This weak restoring circumvents the surface salinity drift that would occur through the lack of any stabilizing feedback if the model is forced with slightly incorrect evaporation, precipitation, and runoff fields.

Two quasi-equilibrium experiments of 1000-year duration were performed with the model. In the first one (CTRL), k_{sant} was set equal to 0.31 W m^{-1} K^{-1}, while in the second one (LC), k_{sant} was reduced to 0.16 W m^{-1} K^{-1}. In both cases, the thermal conductivity of snow on Arctic sea ice was taken equal to 0.31 W m^{-1} K^{-1}. It should be noted that CTRL and the control run of GF are exactly alike. Results discussed below are averages over the last 10 years of integration.

3. Results

Figure 1a depicts the September geographical distribution of ice thickness in the Southern Hemisphere from CTRL. Clearly, there is too little ice between 90° and 160° E and too much in the Bellingshausen Sea. GF attributed these shortcomings to too intense a convection in the Western Pacific Ocean sector and too strong a wind-induced ice convergence along the western side of the Antarctic Peninsula, respectively. The annual mean, area-averaged ice thickness amounts to 95 cm, which is on the high side of observational estimates [e.g., *Wadhams et al.*, 1987]. The

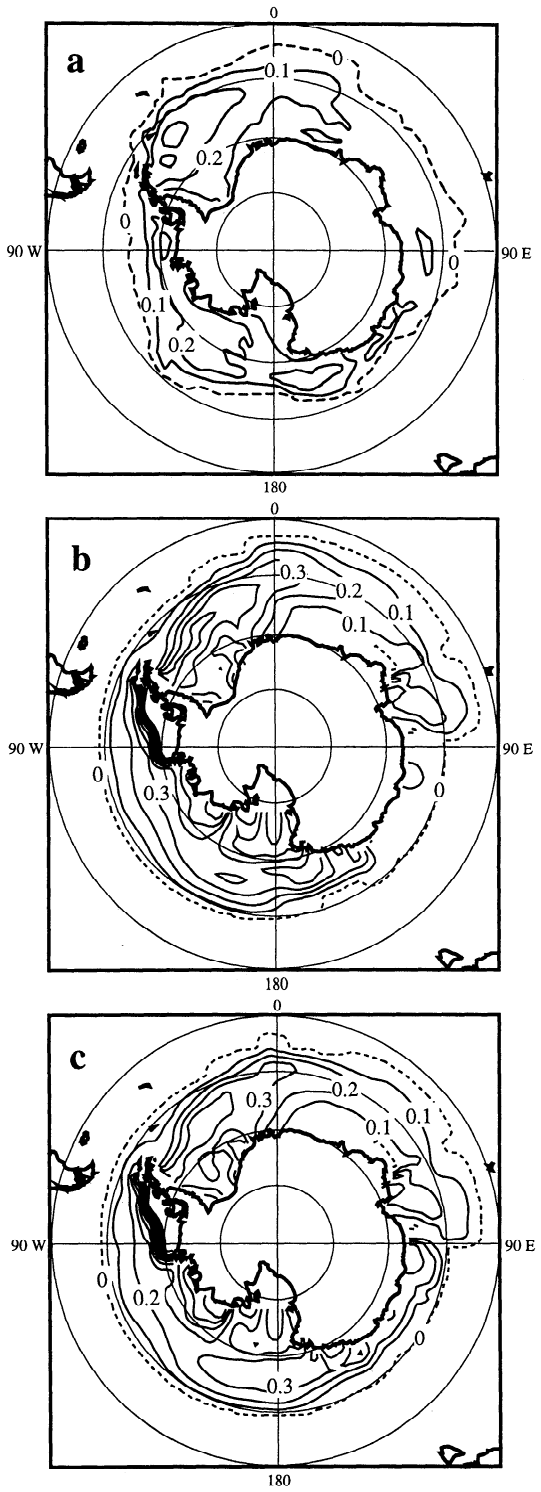

Figure 2. Snow depths on Antarctic sea ice for September (a) as derived from SSM/I data [*Markus and Cavalieri*, 1998], (b) from CTRL, and (c) from LC. Contour interval is 0.1 m.

Table 1. Sector by sector, area-averaged values of the oceanic heat flux at the ice base for September from CTRL and LC. Units are W m^{-2}

Experiment	Weddell Sea (60° W - 20° E)	Amundsen-Bellingshausen Seas (130° W - 60° W)	Ross Sea (160° E - 130° W)	Western Pacific Ocean (90° E - 160° E)	Indian Ocean (20° E - 90° E)
CTRL	26.7	8.1	29.0	30.8	33.5
LC	20.4	7.7	27.0	17.6	32.8

reader is referred to GF for a comparison of the simulated and observed ice extents.

The snow depths on Antarctic sea ice for September as derived from special sensor microwave/imager (SSM/I) data [*Markus and Cavalieri*, 1998] and from CTRL are displayed in Figures 2a and 2b, respectively. The observed depth patterns are reasonably well reproduced by the model, but the modeled snow cover is too thick nearly everywhere. Overall, the computed snow dephts are more realistic than those obtained by *Wu et al.* [1999], the latter being maximum (more than 30 cm) at almost all longitudes along the coastline. This mainly arises from the fact that our sea ice model is forced by climatological precipitation rates. Although far from being perfect, these precipitation rates are more accurate than those generated by the atmospheric general circulation models currently used in climate studies.

The direct effect of a decrease in the snow thermal conductivity is an enhanced insulation of the sea ice from the atmosphere. This weakens the conductive heat flux through the ice and hence reduces ice growth. Let us assume snow and ice thicknesses of 0.2 and 1 m, respectively, and an air-water temperature difference of −15°C (which are typical values for the winter Antarctic environment). From a zero-layer sea ice model with fixed oceanic heat flux, we can estimate that a diminution of k_{sant} from 0.31 to 0.16 W m^{-1} K^{-1} will lead to a decrease in ice freezing of ~20 cm over a 6-month growth season. The differences in September ice thickness between our experiments (Figure 1b) are of the order of this figure over most of the Southern Ocean. However, increases in ice thickness are observed at several locations in the Weddell Sea (up to 10 cm) and between 90° and 160°E (up to 60 cm). We will come back to these peculiarities later on. In LC, the annual mean, area-averaged ice thickness and the annual mean ice volume are reduced by 10 cm (10%) and 1.2×10^3 km^3 (12%), respectively. The maximum ice extent experiences almost no change (as in *Wu et al.* [1999]), but the minimum ice extent is decreased by 0.5×10^6 km^2 (12%).

As the ice cover is thinner in LC than in CTRL, the isostatic balance between snow and sea ice is altered, and more snow ice is produced (the snow ice formation rate is increased by 1 cm per year (4%), on average, in LC), thereby partly counteracting the initial ice thinning. Therefore less snow is generally present on top of sea ice in LC (Figure 2c), so that the simulated snow depths are in better agreement with observations. Note, however, that the snow depth increases between 90° and 160° E in unison with ice thickness and concentration. In both experiments, Antarctic sea ice is snow covered throughout the year. As a consequence, the surface albedo of the pack in LC changes very little.

The reduction in ice growth rate inevitably implies a decrease in the amount of brine released into the ocean. In LC, the annual mean sea surface salinity drops by ~0.1 psu southward of 50° S. The upper ocean being less dense, the convective activity weakens. Less warm deep water is therefore entrained into the surface layer and the sensible heat flux from the ocean to the ice is accordingly diminished, thus lessening or even overcoming the original perturbation. In September, the decrease in oceanic heat flux is particularly pronounced in the Weddell Sea and Western Pacific Ocean sectors (Table 1). It is in these regions that increases in ice thickness are noticed (see Figure 1b). Interestingly enough, the Weddell Sea areas where ice thickens in LC coincide exactly with the locations where, according to data analysis made by *Martinson and Iannuzzi* [1998], small variations in ice growth could modify drastically the structure of the water column. Between 90° and 160° E, the enhanced stability of the water column resulting from the lower sea surface salinity allows ice to remain and hence leads to an improved ice thickness distribution. Although mixing is also weakened over shallow continental shelves, the vertical temperature variation is not sufficient to significantly change the oceanic heat flux there.

The above-mentioned alterations noticeably affect the World Ocean thermohaline circulation and water mass properties. From Figure 3, it can be seen that the intensity of the meridional overturning cell close to Antarctica decreases by 3.5 Sv (10%; 1 Sv = 10^6 m^3 s^{-1}) in LC. As a result, the export of Antarctic Bottom Water (AABW) into the Atlantic basin is reduced by 0.3 Sv (5%). A concomitant increase of 1.8 Sv (10%) in the amount of North Atlantic Deep Water (NADW) exported into the model Southern Ocean is observed. Compared to CTRL, the global deep ocean is warmer by 0.1°C. This warming is caused by the weakening of the Southern Ocean convective activity and by the partial replacement of the cold AABW by relatively warm NADW.

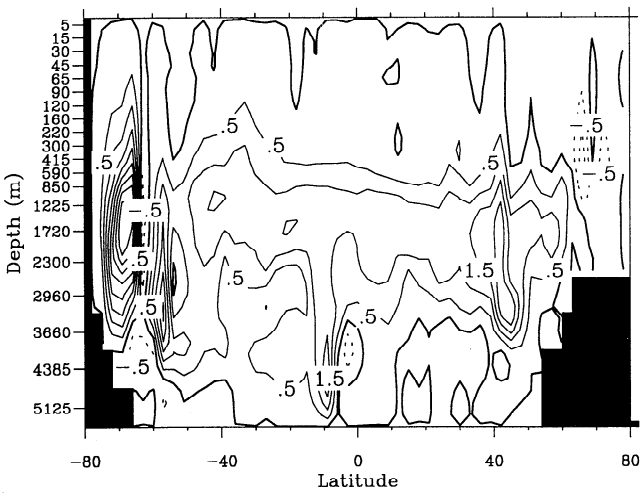

Figure 3. Differences in annual mean, zonally integrated meridional overturning streamfunction between LC and CTRL. Contour interval is 0.5 Sv (1 Sv = 10^6 m^3 s^{-1}). Flow is clockwise around solid contours.

4. Conclusions

We have assessed the impact of using in a global, coarse-resolution ice-ocean model a value for k_{sant} of 0.16 W m^{-1} K^{-1} instead of 0.31, based on field measurements recently carried out in the eastern sector of the Southern Ocean and in the Bellingshausen, Amundsen, and Ross Seas. The immediate effect is a weakening of the vertical conduction of heat through the snow-ice system and an accompanying decrease in ice growth rate. Less brine is therefore rejected into the ocean and the Southern Ocean stratification strengthens, thus leading to a smaller oceanic heat flux at the ice bottom. This in turn moderates the decrease in ice growth. At some locations in the Weddell Sea and in Western Pacific Ocean sector, the reduction in oceanic heat flux is so strong that sea ice actually thickens. Also, as a result of the reduced convective activity, the AABW formation rate decreases and the global deep ocean slightly warms.

Reducing k_{sant} by half somewhat improves the geographical distributions of snow and ice thicknesses in the model Southern Hemisphere and yields a decrease in the average thickness of the Antarctic ice pack of 10 cm (10%). This overall response is much weaker than that obtained by *Wu et al.* [1999] with an atmosphere–sea ice general circulation model. In their case, the reduction in ice thickness averaged 20 cm (27%). Since their study did not include the aforementioned negative oceanic feedback and ours does not account for important positive atmospheric feedbacks (such as the albedo-temperature feedback), the actual sensitivity is very likely between the two estimates.

Our results confirm the importance of correctly representing the insulating effect of snow in large-scale sea ice models. Only sparse field measurements of snow thermal conductivity have been performed so far. It is hoped that more extensive data will be collected in the near future, so that a comprehensive parameterization suited for global climate models can be developed.

Acknowledgments. We wish to thank M. A. Morales Maqueda and two anonymous referees for their careful reading of the manuscript and constructive criticism. T. Fichefet and H. Goosse are Research Associate and Senior Research Assistant at the National Fund for Scientific Research (Belgium), respectively. This study was done within the scope of the Global Change and Sustainable Development Programme (Belgian State, Prime Minister's Services, Federal Office for Scientific, Technical, and Cultural Affairs, Contract CG/DD/09A) and the Concerted Research Action 097/02-208 (French Community of Belgium, Department of Education, Research, and Formation). All of this support is gratefully acknowledged.

References

Baumgartner, A., and E. Reichel, *The World Water Balance*, 179 pp., Elsevier, New York, 1975.

Berliand, M. E., and T. G. Strokina, *Global Distribution of the Total Amount of Clouds* (in Russian), 71 pp., Hydrometeorological, Leningrad, Russia, 1980.

Crutcher, H. L., and J. M. Meserve, Selected level heights, temperature and dew points for the Northern Hemisphere, *NAVAIR Rep. 50-1C-52*, revised, U. S. Nav. Weather Serv. Command, Washington, D. C., 1970.

Eicken, H., H. Fischer, and P. Lemke, Effects of the snow cover on Antarctic sea ice and potential modulation of its response to climate change, *Ann. Glaciol.*, *21*, 369-376, 1995.

Fichefet, T., and M. A. Morales Maqueda, Sensitivity of a global sea ice model to the treatment of ice thermodynamics and dynamics, *J. Geophys. Res.*, *102*, 12,609-12,646, 1997.

Fichefet, T., and M. A. Morales Maqueda, Modelling the influence of snow accumulation and snow-ice formation on the seasonal cycle of the Antarctic sea-ice cover, *Clim. Dyn.*, 15, 251-268, 1999.

Goosse, H., and T. Fichefet, Importance of ice-ocean interactions for the global ocean circulation: A model study, *J. Geophys. Res.*, 104, 23,337-23,355, 1999.

Grabs, W., T. De Couet, and J. Pauler, Freshwater fluxes from continents into the world oceans based on the data of the global runoff data base, *Global Runoff Data Centre Rep. 10*, 228 pp., Fed. Inst. of Hydrol., Koblenz, Germany, 1996.

Hellerman, S., and M. Rosenstein, Normal monthly wind stress over the World Ocean with error estimates, *J. Phys. Oceanogr.*, 13, 1093-1104, 1983.

Ledley, T. S., Snow on sea ice: Competing effects in shaping climate, *J. Geophys. Res.*, *96*, 17,195-17,208, 1991.

Levitus, S., Climatological atlas of the world ocean, *NOAA Prof. Pap. 13*, 173 pp., U. S. Gov. Print. Office, Washington, D. C., 1982.

Markus, T., and D. J. Cavalieri, Snow depth distribution over sea ice in the Southern Ocean from satellite passive microwave data, in *Antarctic Sea Ice: Physical Processes, Interactions and Variability, Antarc. Res. Ser.*, vol. 74, edited by M. O. Jeffries, pp. 19-39, AGU, Washington, D. C., 1998.

Martinson, D. G., and R. A. Iannuzzi, Antarctic ocean-ice interaction: Implications from ocean bulk properties distribution in the Weddell Gyre, in *Antarctic Sea Ice: Physical Processes, Interactions and Variability, Antarc. Res. Ser.*, vol. 74, edited by M. O. Jeffries, pp. 243-271, AGU, Washington, D. C., 1998.

Massom, R. A., V. I. Lytle, A. P. Worby, and I. Allison, Winter snow cover variability on East Antarctica sea ice, *J. Geophys. Res.*, *103*, 24,837-24,855, 1998.

Maykut, G. A., and N. Untersteiner, Some results from a time-dependent thermodynamic model of sea ice, *J. Geophys. Res.*, *76*, 1550-1575, 1971.

Mellor, G. L., and T. Yamada, Development of a turbulence closure model for geophysical fluid problems, *Rev. Geophys. Space Phys.*, 204, 851-875, 1982.

Owens, W. B., and P. Lemke, Sensitivity studies with a sea ice–mixed layer–pycnocline model in the Weddell Sea, *J. Geophys. Res.*, *95*, 9527-9538, 1990.

Taljaard, J. J., H. van Loon, H. L. Crutcher, and R. L. Jenne, Climate of the upper air, I, Southern Hemisphere, vol. 1, Temerature, dew points, and heights at selected pressure levels, *NAVAIR Rep. 50-1C-55*, 135 pp., U. S. Nav. Weather Serv. Command, Washington, D. C., 1969.

Trenberth, K. E., J. G. Olson, and W. G. Large, A global ocean wind stress climatology based on ECMWF analyses, *National Center for Atmos. Res. Tech. Note*, NCAR/TN-338+STR, 93 pp., 1989.

Semtner, A. J., Jr., A model for the thermodynamic growth of sea ice in numerical investigations of climate, *J. Phys. Oceanogr.*, *6*, 379-389, 1976.

Sturm, M., K. Morris, and R. Massom, The winter snow cover of the West Antarctic pack ice: Its spatial and temporal variability, in *Antarctic Sea Ice: Physical Processes, Interactions and Variability, Antarc. Res. Ser.*, vol. 74, edited by M. O. Jeffries, pp. 1-18, AGU, Washington, D. C., 1998.

Wadhams, P., M. A. Lange, and S. F. Ackley, The ice thickness distribution across the Atlantic sector of the Antarctic Ocean in midwinter, *J. Geophys. Res.*, *92*, 14,535-14,552, 1987.

Wu, X., W. F. Budd, V. I. Lytle, and R. A. Massom, The effect of snow on Antarctic sea ice simulations in a coupled atmosphere-sea ice model, *Clim. Dyn.*, *15*,127-143, 1999.

Xie, P., and P. A. Arkin, Analyses of global monthly precipitation using gauge observations, satellite estimates and numerical model predictions, *J. Clim.*, *9*, 840-858, 1996.

T. Fichefet, B. Tartinville, H. Goosse, Institut d'Astronomie et de Géophysique G. Lemaître, Université Catholique de Louvain, 1348 Louvain-la-Neuve, Belgium. (e-mail: fichefet@astr.ucl.ac.be)

(Received September 13, 1999; accepted December 09, 1999.)